THE ASTRONOMICAL JOURNAL, IN PRESS
Preprint typeset using LaTeX style emulateapj v. 26/01/00

STELLAR POPULATION VARIATIONS IN THE MILKY WAY'S STELLAR HALO

ERIC F. BELL[1], XIANG XIANG XUE[2,3], HANS-WALTER RIX[2], CHRISTINE RUHLAND[2], DAVID W. HOGG[4,2]
[1] Department of Astronomy, University of Michigan, 500 Church St., Ann Arbor, MI 48109, USA; ericbell@umich.edu
[2] Max-Planck-Institut für Astronomie, Königstuhl 17, D-69117 Heidelberg, Germany
[3] Key Laboratory of Optical Astronomy, National Astronomical Observatories, CAS, 20A Datun Road, Chaoyang District, 100012, Beijing, China
[4] Center for Cosmology and Particle Physics, Department of Physics, New York University, 4 Washington Place #424, New York, NY 10003, USA

THE ASTRONOMICAL JOURNAL, IN PRESS

ABSTRACT

If the stellar halos of disk galaxies are built up from the disruption of dwarf galaxies, models predict highly structured variations in the stellar populations within these halos. We test this prediction by studying the ratio of blue horizontal branch stars (BHB stars; more abundant in old, metal-poor populations) to main-sequence turn-off stars (MSTO stars; a feature of all populations) in the stellar halo of the Milky Way using data from the Sloan Digital Sky Survey. We develop and apply an improved technique to select BHB stars using *ugr* color information alone, yielding a sample of $\sim$9000 $g < 18$ candidates where $\sim 70\%$ of them are BHB stars. We map the BHB/MSTO ratio across $\sim 1/4$ of the sky at the distance resolution permitted by the absolute magnitude distribution of MSTO stars. We find large variations of BHB/MSTO star ratio in the stellar halo. Previously identified, stream-like halo structures have distinctive BHB/MSTO ratios, indicating different ages/metallicities. Some halo features, e.g., the low-latitude structure, appear to be almost completely devoid of BHB stars, whereas other structures appear to be rich in BHB stars. The Sagittarius tidal stream shows an apparent variation in BHB/MSTO ratio along its extent, which we interpret in terms of population gradients within the progenitor dwarf galaxy. Our detection of coherent stellar population variations between different stellar halo substructures provides yet more support to cosmologically motivated models for stellar halo growth.

Subject headings: galaxies: evolution — galaxies: bulges — galaxies: spiral — galaxies: general — galaxies: stellar content

1. INTRODUCTION

Over the last decade, it has become clear that a sizeable, perhaps dominant, part of the stellar halo of the Milky Way is composed of the accumulated debris from the disruption of distinct satellite galaxies. Starting with the discovery and characterization of the tidal debris from the disruption of the Sagittarius dwarf galaxy (Ibata et al. 1995; Majewski et al. 2003), a variety of other stellar halo overdensities have been discovered: the low-latitude stream (Yanny et al. 2003; Ibata et al. 2003), the Virgo and Hercules-Aquila overdensities (Duffau et al. 2006; Jurić et al. 2008; Belokurov et al. 2007a), and a number of smaller tidal streams (Odenkirchen et al. 2001; Grillmair 2006; Grillmair & Dionatos 2006; Grillmair & Johnson 2006; Belokurov et al. 2007b; Grillmair 2009; Newberg, Yanny & Willett 2009). Models of stellar halos that formed in a cosmological context through the disruption of dwarf galaxies have been developed and refined (Bullock et al. 2001; Bullock & Johnston 2005; Abadi et al. 2006; Cooper et al. 2010), providing quantitative predictions for the structure and stellar content of stellar halos formed in such a fashion. Remarkably, the structure and degree of substructure of the model stellar halos appear to be in quantitative agreement with observations of the Milky Way's stellar halo (Bullock & Johnston 2005, Bell et al. 2008): stellar halos with $\sim 10^9 L_\odot$, a roughly r^{-3} density profile, and showing rich substructure on a variety of spatial scales.

A clear prediction of such a picture is that any population differences in the stellar halo, arising from different progenitor populations, should have a similar morphology to the stellar density inhomogeneities. The metallicity–mass correlation of satellite galaxies will translate into variations in stellar halo metallicity, as debris from larger satellites will have higher metallicity than those of lower-luminosity satellites or globular clusters. Furthermore, one expects to see distinctive signatures in age and detailed element abundance patterns, reflecting when satellites were accreted (Robertson et al. 2005, Font et al. 2006; see also Tumlinson 2010). Signatures of population inhomogeneity have been detected: hints of chemical signatures of kinematically-detected local streams (e.g., Helmi et al. 2006), small variations in metallicity within the nearby parts of the stellar halo, especially associated with the low-latitude stream (e.g. Ivezić et al. 2008)[1], the tendency for the halo to have metal-poorer stars at larger radii (e.g., Carollo et al. 2007), and a recent color–magnitude diagram (CMD) fitting analysis of Sloan Digital Sky Survey (SDSS) stripes showing both a radial metallicity gradient and large density and metallicity variations around that gradient (de Jong et al. 2010). Yet, for the most part, the observational signatures of such population variations are accessible for relatively bright stars only (high S/N *ugriz* imaging, or moderate S/N spectra). Accordingly, those radii in our own stellar halo where substructure is rich ($10 < r < 40$ kpc) are not probed particularly well. Some of the most impressive evidence for stellar halo population variations are from M31, where significant variations in stellar age and metallicity have been documented (Brown et al. 2006; Richardson et al. 2008). In particular, Ibata et al. (2007) and McConnachie et al. (2009) have used the color of the red giant branch stars (practically inaccessible in the Milky Way's halo because distances are uncertain) to provide panoramic views of the stellar populations in the M31 halo, showing clearly that stellar population variation

[1] A particular concern in this case is that the low-latitude stream may have a significant or even dominant contribution from the debris torn off of the Milky Way disk; thus, the detection of a distinctive population may result from disk debris superimposed on a relatively homogeneous stellar halo.

can be associated with particular substructures.

In this paper, we present an exploration of stellar population variations and their morphology within the stellar halo of the Milky Way. We make use of the ratio of blue horizontal branch (BHB) stars to main-sequence turn-off (MSTO) stars as our main observational diagnostic of stellar population variations. While the exact conditions under which BHB stars develop are not completely clear (post-main sequence-stars with core helium burning and hydrogen shell burning, with relatively low hydrogen envelope masses; Hoyle & Schwarzschild 1955), studies of globular clusters demonstrate that they signpost particularly ancient and metal-poor stellar populations. We take MSTO stars (present in all populations) as a proxy for the general stellar content of the halo; thus, variations in BHB to MSTO ratio qualitatively probe the ratio of ancient and metal poor stars to all stars. Despite our lack of a complete understanding of which populations harbor BHB stars, these stars are in many other respects ideal probes of population variations in the stellar halo: they can be selected from the SDSS imaging and spectroscopic dataset, they are relatively luminous (allowing probing to large distances), and they are nearly standard candles.

We outline and apply an improved color selection method to isolate a sample of over 9000 $g \lesssim 18$ high-probability BHB star candidates from SDSS data (§2). The MSTO stars are color-selected in a simple empirical fashion to encompass the full range of MSTO colors in the stellar halo; we therefore use MSTO stars as a proxy for the general stellar content of the stellar halo. We then explore the relative distributions of BHB to MSTO stars in the Heliocentric distance range $5 \lesssim r/\mathrm{kpc} \lesssim 30$ across $\sim 1/4$ of the celestial sphere, providing a panoramic view of stellar population variations in the Milky Way's stellar halo (§3). Owing to our uncertainty in the exact conditions under which BHB stars form, such a view of stellar population variations is necessarily qualitative in nature, but has the advantage that stellar population variations can be traced out to larger distances than is currently possible with complementary tracers (e.g., the lower main sequence stars of Ivezić et al. 2008). We then compare qualitatively with models of stellar halos built entirely through the disruption of dwarf galaxies (§4), and explore some other implications of our results (§5).

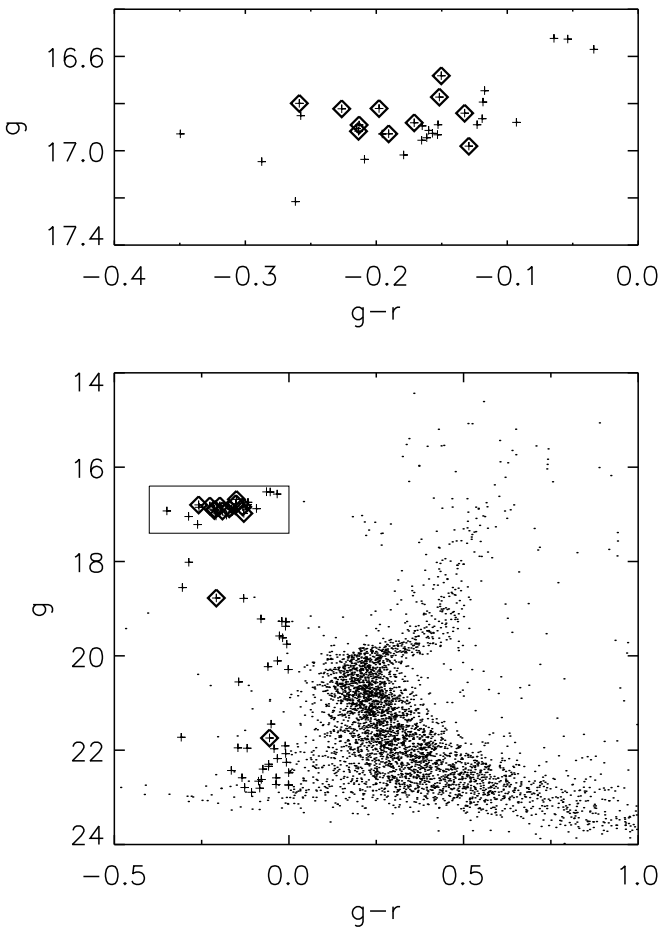

FIG. 1.— Illustration of the recovery of BHB stars for the globular cluster NGC 5024. The bottom panel shows the cluster CMD over a wide range of colors and magnitudes; the top panel zooms into the area richest in BHB stars. Stars selected as BHB candidates by $-0.5 < g-r < 0$ and $0.8 < u-g < 1.6$ are shown as crosses, while those with $> 50\%$ probability of being a BHB star as estimated by our method are marked with an additional diamond.

2. BHB AND MSTO STAR SAMPLES

We use publicly available catalogs derived from the Sloan Digital Sky Survey's (SDSS) Data Release Seven (DR7; Abazajian et al. 2009) to select BHB and MSTO stars for further study. The SDSS is an imaging and spectroscopic survey that has so far mapped $\sim 1/4$ of the sky. Imaging data are produced simultaneously in five photometric bands, namely *u*, *g*, *r*, *i*, and *z* (Fukugita et al. 1996; Gunn et al. 1998; Hogg et al. 2001; Gunn et al. 2006). The data are processed through pipelines to measure photometric and astrometric properties (Lupton et al. 1999; Stoughton et al. 2002; Smith et al. 2002; Pier et al. 2003; Ivezić et al. 2004; Tucker et al. 2006) and to select targets for spectroscopic follow-up (Blanton et al. 2003; Strauss et al. 2002).

To obtain full area coverage and maximal distance range, we must rely on BHB star samples selected by *ugr* color information alone. One of the well-known practical challenges of using BHB stars for stellar halo science is that genuine BHB stars are outnumbered by intrinsically fainter blue straggler stars (as discussed at length by Kinman, Suntzeff & Kraft 1994, Wilhelm, Beers & Gray 1999, Clewley et al. 2002, Sirko et al. 2004, Kinman et al. 2007, and Xue et al. 2008; some authors refer to these as a blue plume, e.g., Bellazzini et al. 2006a). Fig. 1 illustrates this issue[2], showing BHB stars at $g \sim 16.85$ and less luminous blue straggler stars with similar colors at $18 \lesssim g \lesssim 20$. These blue straggler stars are a common feature of globular clusters, dwarf galaxies and the stellar halo (e.g., Sandage 1953; Bellazzini et al. 2006a; Preston & Sneden 2000; Carney et al. 2001). Blue stragglers are somewhat enigmatic, as they are intermediate mass main sequence stars in (old) populations where the MSTO is at lower masses. It is thought that there are at least two possible formation routes: stellar collisions in dense star clusters (Hills & Day 1976), and mass transfer in the evolution of close binaries (McCrea 1964, or potentially in triple star systems; Perets & Fabrycky 2009) in low-density environments (where the latter low stellar density route is more relevant here; see, e.g., Preston & Sneden 2000, Mathieu & Geller 2009, Knigge, Leigh & Sills 2009).

[2]Because NGC 5024 is particularly BHB star rich, the blue stragglers do not dominate in this figure. When translated to the global halo population, and accounting for the stellar halo density profile and different distances of BHB and blue straggler stars at a given magnitude, BHB stars are typically outnumbered by a significant factor by blue stragglers.

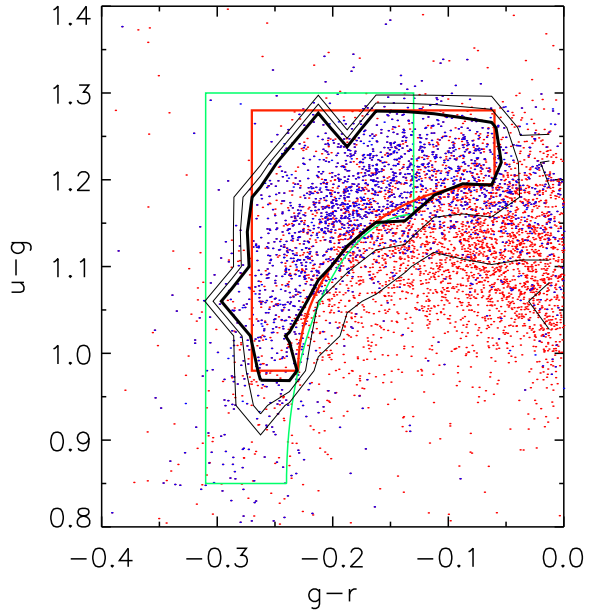

FIG. 2.— Illustration of the BHB star selection method which identifies the optimal BHB selection region in the $u-g$ vs. $g-r$ color plane using extensive spectroscopic identification using the SDSS. Only stars with spectroscopic identifications are shown. Stars that are argued to be BHB stars on the basis of their spectra by Xue et al. (2008) are shown in blue. Contours show the fraction of candidates determined to be BHB stars (contours are 10%, 30% and 50%; the 50% contour is thicker than the others). In what follows we consider BHB stars within the 50% contour only. Overplotted are our approximation to the BHB color selection limits (red), and the 'stringent' color cut of Sirko et al. (2004, green).

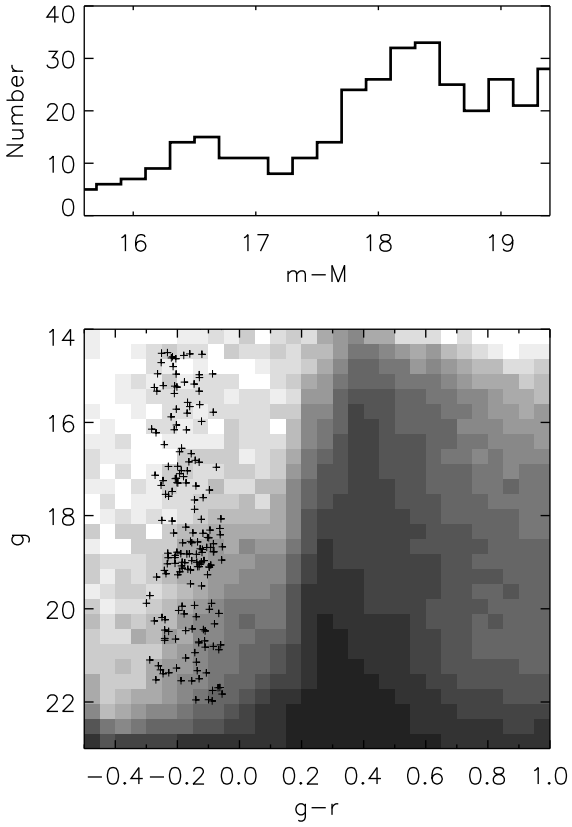

FIG. 3.— BHB star candidates in the direction of RA/Dec=(204,5). The lower panel shows the logarithmic density of stars in the CMD in gray scale in an area of radius 4°, with those stars identified as BHB candidates on the basis of their *ugr* colors being shown with crosses. The upper panel shows the distance modulus distribution of BHB candidates along this line of sight, showing two overdensities; the more distant of these at $m-M \sim 18.3$ is part of the tidal tail from Sagittarius. It is worth noting that blue straggler contamination has a much broader absolute magnitude distribution; the confinement of this overdensity to such a small apparent magnitude range is further evidence that the sample is dominated by BHB stars (that have a small range in absolute magnitude).

2.1. *Color selection of BHB stars*

Choosing stars in the broad color cut broad cuts $-0.5 < g-r < 0$ and $0.8 < u-g < 1.6$ gives a sample that is $\gtrsim$3:1 blue stragglers to BHB stars for the full $g \lesssim 19.5$ sample of Xue et al. (2008), and 60% blue stragglers for the $g \lesssim 18$ subsample of interest in this paper. This ratio is based entirely on the sample of stars with SDSS spectroscopy as reported in Xue et al. (2008). The algorithm used to select stars for SDSS spectroscopy changed a number of times during the survey, and does not select uniformly in color-color space; these contamination fractions are affected by this selection (we present alternative estimates of contamination fractions derived in other ways later). Yet, it is clear that such a level of contamination is a significant challenge for quantitative analysis of the BHB star population using photometry alone.

Our goal here is to combine the extensive SDSS spectroscopy with SDSS photometry to devise color selection criteria that are significantly improved in their trade-off between BHB purity and sample size (similar in spirit to the 'stringent' color cut of Sirko et al. 2004; see also Clewley et al. 2005 and Kinman et al. 2007 for selection of BHB stars from *ugr* photometry). Using a calibration sample of BHB star candidates with spectra (Xue et al. 2008, following the methodology of Sirko et al. 2004), we have determined the probability that a BHB candidate with given $u-g$ and $g-r$ color is a spectroscopic BHB star; the rest of the candidates are other blue stars, and are presumably mostly blue stragglers. Fig. 2 illustrates this process, showing stars with $g < 18$ (appropriate for BHB stars in the Heliocentric distance range considered here) and with spectra from the SDSS (Xue et al. 2008). Blue data points show stars that are very likely to be BHB stars on the basis of their spectra (a contamination of much less than 10% has been argued by Xue et al. 2008 and Sirko et al. 2004 at these $g < 18$ limits). The thick contour outlines the region of color-color space where the fraction of BHB candidates that are spectroscopically-classified BHB stars is $> 50\%$ and there were more than 16 stars in a bin of 0.025×0.04 mag (to ensure a high enough number of stars to measure the BHB star fraction with some fidelity). This region is well-approximated by the selection region shown in red in Fig. 2: $0.98 < u-g < 1.28$, $-0.2 < g-r < -0.06$ and excluding the region with $([u-g-0.98]/0.215)^2+([g-r+0.06]/0.17)^2 < 1$ (formulated similarly to the 'stringent' color cut of Sirko et al. 2004, shown in green).

2.2. *Completeness and contamination of color-selected samples*

We first quantify the likely completeness and contamination of the color-selected $g < 18$ sample that is the main focus of this paper. We estimate the completeness and contamination in two ways: using the spectroscopic sample, and independent spot checking on BHB star-rich globular clusters.

Our primary estimate of contamination and completeness comes from the spectroscopic training sample used to determine the color cuts. Given the average spectroscopic completeness within the $> 50\%$ contour, and weighted by the number of stars in our photometric catalog per bin in color-color space (this to a certain extent corrects for the non-uniform color selection of stars with SDSS spectra), we expect $\sim 67-74\%$ of the BHB candidates within the selection region to be real BHB stars (where the two ends of the range assume that 90% to 100% of the spectroscopic BHB stars are actually BHB stars, following Sirko et al. 2004 and Xue et al. 2008). Furthermore, we find that the color cuts select $\sim 60\%$ of the BHB stars in the spectroscopic sample.

Secondary estimates of contamination and completeness are possible through the investigation of BHB stars in globular clusters and dwarf galaxies. This method has the advantage that an independent indicator of the nature of the stars is available through their position on the CMD, but have the disadvantage that there are very few clusters in the relevant distance range, and that the number of BHB stars per cluster is typically very modest (dwarf galaxies were also tested, but are more distant, and give results qualitatively consistent with the picture presented here but are of limited quantitative use). In Fig. 1, we illustrate this method to the BHB star-rich globular cluster NGC 5024. Stars selected as BHB candidates by the broad cuts $-0.5 < g-r < 0$ and $0.8 < u-g < 1.6$ are shown as crosses, while those with $> 50\%$ probability as estimated by our method are shown as diamonds. There are 30 actual BHB stars in this sample at the distance of NGC 5024 (defined as having $-0.4 < g-r < 0$ and $16.6 < g < 17.1$); our method recovers 11 of them with only 2 contaminants (i.e., a completeness of $\sim 37\%$ and a contamination of $\sim 15\%$, consistent with our expectation of $\lesssim 30\%$ contamination). There are indications that NGC 5024 may have an unusually low fraction of recovered stars; NGC 5053 has 5/7 ($\sim 70\%$) BHB stars recovered (with no contaminants).

Considering both tests together, we conclude that this procedure, when applied to $g < 18$ stars with SDSS-quality photometry, gives a sample of $\sim 50\%$ of the real BHB star population with $\lesssim 30\%$ contamination, a considerable improvement over the $\sim$60% contamination given by much more simplistic photometric cuts.

While in this paper we restrict our attention to BHB stars with $g \lesssim 18$, we characterize the likely performance of these cuts for fainter samples with colors characteristic of BHB stars. To estimate the run of photometric uncertainty as a function of measured apparent magnitude in *u*, *g* and *r*-bands, we used repeat imaging of the SDSS stripe 82 as tabulated by Bramich et al. (2008). We then imposed the typical uncertainties of stars with BHB colors at $g \sim 19$ and $g \sim 20$ on the sample of real $g < 18$ stars used to derive the BHB star selection, and checked how the fraction of the real BHB stars that are recovered, and the contamination by BS stars, should depend on apparent magnitude. Recall for the $g < 18$ stars, the recovery/contamination fractions for the spectroscopic sample are (60%, 25%), i.e., the cut isolates 60% of the population with only 25% contamination. For $g = 19$ and $g = 20$, our estimates of the recovery/contamination fractions are (40%, 40%) and (20%, 50%) respectively, i.e., at $g = 19$ the situation is improved over the 60% contamination in the broad $-0.5 < g-r < 0$, $0.8 < u-g < 1.6$ color bin by applying the cuts described here, but at $g = 20$ the cuts throw out most of the genuine BHB stars without improving contamination significantly. These fractions are consistent with our investigations of the performance of cuts on more distant BHB-rich targets, e.g., the Sextans or Draco dwarf galaxies (1/4 of the BHB stars recovered, at $g \sim 20$).

2.3. *Estimates of BHB star absolute magnitude*

We estimate the absolute magnitudes for the BHB star candidates by interpolating the $g-r$-dependent M_g calibration from Table 2 of Sirko et al. (2004) with [Fe/H]= −1 (the [Fe/H]= −2 Sirko et al. 2004 calibration is different by < 0.03 mag). Tests of the quality of this calibration are encouraging; the rms of the color-derived absolute magnitudes of BHB stars in globular clusters is ~ 0.1 mag (a measure of the absolute magnitude scatter at a single metallicity), and the overall distance modulus estimates of the clusters and dwarf galaxies agree with those determined by independent means to $\lesssim 0.1$ mag (a rough constraint on the degree of metallicity dependence of the BHB absolute magnitude calibration; these results are reported in full in Ruhland et al. 2010).

We also compared the calibration of BHB absolute magnitude from Sirko et al. (2004) with the metallicity-dependent BHB star models from Dotter et al. (2007) and Dotter et al. (2008). These models make use of more realistic input physics than the modeling from Sirko et al. (2004); however, the *ugr* colors of BHB stars from Dotter et al. (2008) do not match the colors of SDSS BHB stars particularly well (they are offset in particular in $u-g$ color by ~ 0.1 mag, and may be offset by a smaller amount in $g-r$ color; in contrast, the more rudimentary modeling by Sirko et al. 2004 was designed to match the colors well). These offsets in color prohibit a quantitative assessment of which stars would fall in the selection region; selecting instead those BHB stars reddest in $u-g$ at a given $g-r$ (a qualitative version of our selection method), corresponding to metallicities of $[\mathrm{Fe/H}] \lesssim -1.5$, gives a full range in $\Delta M_g \lesssim 0.3$ mag at a given $g-r$. Taken together, the tests of absolute magnitude calibration on clusters and dwarf galaxies in conjunction with the Dotter et al. (2008) metallicity-dependent BHB star models paints a picture in which the absolute magnitudes adopted for our BHB candidates are accurate to $\lesssim 0.1$ in overall zero point, and will scatter $\lesssim 0.2$ mag at worst – far less than the ~ 0.9 mag absolute magnitude scatter of our MSTO sample.

The final sample of high-probability BHB stars selected using the 50% color contour in Fig. 2 and with $g < 21$ is more than 14000 stars in the North Galactic Cap selection region we use in this paper ($b > 20$ for $180 < l < 240$, and $b > 30$ for $l \leq 180$ and $l \geq 240$, dictated largely by the SDSS coverage), and more than 9000 stars in the Heliocentric distance range 5–30 kpc (corresponding approximately to $g \lesssim 18$).

2.4. *Selection of MSTO stars, and comparison of MSTO and BHB stars*

Following Bell et al. (2008), we select over 4.3 million MSTO stars in the foreground extinction-corrected color range $0.2 < g-r < 0.4$ and $18 < r < 22$; this color and magnitude range was selected empirically to encompass the most densely-populated bins of color space for the halo MSTO stars (see Fig. 1 of Bell et al. 2008). Examination of globular clusters and model

CMDs demonstrates that MSTO stars selected in this fashion have a roughly Gaussian distribution of absolute magnitudes with a mean $M_r \sim 4.5$ and a rms $\sigma_{mag,MSTO} = 0.9$ (see Fig. 2 of Bell et al. 2008). By choosing a particular color range for MSTO star selection, we are in principle susceptible to changes in the main-sequence stellar population from location to location in the stellar halo (through variation in the metallicity and age). In practice, this turns out to be a minor concern, as the color of the stellar halo MSTO (the blue edge of the turn-off in particular) varies little across the SDSS area; the stellar population in the stellar halo varies little enough that it is essentially undetectable using MSTO color alone.

Fig. 3 illustrates the properties of the stellar sample in a particular line of sight towards the Sagittarius tidal tail. This shows the CMD of (primarily halo) stars in a 4° radius cone around (RA,Dec)=(204,5). MSTO stars in the halo are very numerous, having $0.2 < g-r < 0.4$ and $g > 18$ (brighter MSTO stars with $g < 18$ have $g-r \sim 0.4$, representing more metal-rich thick disk stars). BHB candidates are selected by virtue of their *ugr* colors using the method illustrated in Fig. 2, and are shown as crosses. Because BHB stars have a small scatter in absolute magnitude, BHB star-rich halo overdensities (at $m-M \sim 16.5$ and $m-M \sim 18.3$) are clearly-defined. The corresponding MSTO overdensities, about 4 magnitudes fainter, are not anywhere near as clearly defined owing to the larger spread in MSTO absolute magnitudes. In this paper, we will be analyzing the two populations in concert as an easily-measurable but largely qualitative diagnostic for stellar population variations in the stellar halo of the Milky Way.

3. POPULATION VARIATIONS IN THE STELLAR HALO OF THE MILKY WAY

Analyzing the ratio of BHB to MSTO stars requires that we compare the stars in the same 'effective volume'. We convolve the BHB star distance moduli with a Gaussian with width $\sigma_{mag,MSTO} = 0.9$ mag (referred to hereafter as the degraded BHB sample) to yield the same scatter between degraded distance modulus $(m-M)_{degraded}$ and true $(m-M)_{true}$ as is estimated for the MSTO stars. Then we can compare the 'distance smoothed' distribution of BHB stars, with $(m-M)_{degraded}$, directly and quantitatively to the distribution of MSTO stars with the same $(m-M)_{MSTO}$ range (i.e., BHB stars are compared with MSTO stars that are ∼4 mag fainter)[3]. The results are illustrated in Fig. 4.

Fig. 4 displays various aspects of the comparison between BHB and MSTO star distributions, and we work through them in turn. The center column of panels shows the distribution of MSTO stars in four distance modulus slices: $13.5 \leq m-M < 14.5$, $14.5 \leq m-M < 15.5$, $15.5 \leq m-M < 16.5$, and $16.5 \leq m-M < 17.5$, or distances of $5-8$, $8-13$, $13-20$ and $20-32$ kpc respectively, smoothed in angular position with a Gaussian kernel with $\sigma = 0.5°$. The gray scale shows the number of stars in $0.5° \times 0.5°$ bins with a linear mapping between intensity and stellar density. Black areas lack SDSS DR7 coverage. These panels show various previously described features of the Milky Way stellar halo (e.g., Belokurov et al. 2006; Newberg et al. 2007; Bell et al. 2008): superimposed on a relatively smooth distribution of stars is the Sagittarius stream (e.g., Ibata et al. 1995; Majewski et al. 2003; Belokurov et al. 2006) stretching from the Galactic anticenter ($m-M \sim 16$) to the Galactic center ($m-M \sim 17$). Near the North Galactic Pole (NGP) at $m-M \lesssim 16$ is the diffuse Virgo overdensity (e.g., Duffau et al. 2006; Newberg et al. 2007; Jurić et al. 2008). At $m-M \lesssim 15$ in the Galactic anticenter direction at low galactic latitudes is the low-latitude structure (also referred to as the Monoceros stream; e.g., Newberg et al. 2002; Peñarrubia et al. 2005; Momany et al. 2006). At $l \sim 45°$ and $b \sim 45°$ is the diffuse Hercules-Aquila structure (Belokurov et al. 2007a). One can also see a variety of less prominent features: globular clusters as 'hot pixels', and at $m-M \sim 17$ stretching from $(l,b) \sim (250,50)$ to $(l,b) \sim (160,40)$ is the Orphan Stream (Belokurov et al. 2007b; Grillmair 2006).

In the left-hand column of panels in Fig. 4, we show the BHB star distribution in the same distance bins, and convolved with a distance modulus kernel of width $\sigma_{\rm MSTO} = 0.9$ mag to match the MSTO absolute magnitude scatter; an angular smoothing of $\sigma = 1°$ is applied to suppress the much larger shot noise due to the 100-fold smaller sample. Thus, the left-hand panels reflect BHB star maps of the *same halo distance slices* as the MSTO panels. One can see some similarities, as well as some striking differences, between the distributions of the BHB and MSTO stars. These differences are quantified and illustrated in the right-hand panels, which show a color representation of the BHB to MSTO star ratio. Here, the distributions of BHB and MSTO stars are smoothed by a Gaussian kernel with an angle of $\sigma = 6°$ to increase S/N. A bluish-white color denotes BHB/MSTO ratio of $> 1/50$ and red denotes BHB/MSTO $< 1/100$. The intensity scales with the number of stars (dark shades show regions with few stars, whereas light shades denote regions with many stars). Poisson noise is significant on small scales, but contributes less than 3% on the scale of large structures such as the low-latitude stream. The primary uncertainties are systematic in origin: changing the probability threshold for a BHB star to be included in the sample from 50% to 30% tests the influence of BHB candidate purity and blue straggler contamination on the results. Such a change produces differences of ∼ 10% in relative BHB/MSTO ratio (i.e., variations in the BHB/MSTO from place to place on the map)[4]. Another source of systematic error is possible variations in MSTO absolute magnitude or scatter as a function of position. Fig. 2 of Bell et al. (2008) shows that there are some variations in MSTO absolute magnitude and rms from globular cluster to globular cluster, driven by differences in stellar population age/metallicity. Such variations may be present in the stellar halo. We have tested the influence of potential variations in MSTO absolute magnitude (a $\lesssim$ 15% effect in BHB/MSTO ratio for variations in MSTO absolute magnitude of 0.5 mag or less) and scatter in the luminosity of MSTO stars (a few percent effect in BHB/MSTO ratio for 20% changes in the assumed MSTO scatter).

The right set of panels in Fig. 4 demonstrate clearly the key result of this paper: there are significant variations in the BHB/MSTO ratios in the stellar halo of the Milky Way. Perhaps more importantly, these variations coincide spatially with different known halo structures, as expected if the various overdensities were composed of the debris from the disruption of

[3]It should be noted that this shift in magnitude is important also when considering blue straggler contamination. Blue stragglers are 1-3 mag fainter than BHB stars, therefore any blue straggler star contamination should show up at larger equivalent distance modulus (because the blue stragglers are being treated as brighter BHB stars).

[4]Of course, the absolute BHB/MSTO ratio changes by 30%, as the number of BHB star candidates included in the analysis is increased by reducing the BHB probability threshold; such a change in absolute ratio is not important for our purposes.

individual progenitors. Some prominent structures (e.g., the low-latitude structure) appear to be almost completely devoid of BHB stars (as illustrated by the red band at low galactic latitudes in the Galactic anticenter direction in the upper right-hand panel of Fig. 4; BHB/MSTO $\sim 1/90$). Other structures, e.g., the Virgo overdensity at $l \sim 300^\circ$ and $b \sim 70^\circ$ or the Hercules-Aquila overdensity at $l \sim 45^\circ$ and $b \sim 45^\circ$, appear to be considerably richer in BHB stars (both structures have BHB/MSTO $\sim 1/40$). Such differences are highly significant; recalling that the primary uncertainties are systematic, we find that Virgo and Hercules-Aquila are a factor of 2 to 2.5 richer in BHB stars than the low-latitude structure (where the range includes the effects of the random and systematic uncertainties discussed above). Strikingly, parts of the Sagittarius tidal stream (near the NGP and at $m-M \sim 17$) appear to be relatively rich in BHB stars (BHB/MSTO $\sim 1/55$), while the part at $m-M \sim 16$ and $l \sim 200^\circ$ and $b \sim 50^\circ$ is considerably poorer in BHB stars (BHB/MSTO $\sim 1/80$), implying a population gradient along the stream.

Fig. 4 also shows that contamination of the BHB sample by blue stragglers would not affect our key result. Areas with already low BHB/MSTO ratios (the low-latitude stream and parts of Sagittarius) would imply even lower BHB/MSTO in the presence of blue straggler contamination. Furthermore, even for structures such as Virgo or Hercules-Aquila, the association of BHB stars to particular structures already present in MSTO stars (and their having characteristic BHB/MSTO ratios) implies that blue straggler contamination has a small effect, at least for $m-M \lesssim 17.5$. The only possible exception to this is the BHB star-rich section of Sagittarius, which lies in a similar area of the sky and 1-2 magnitudes more distant than the BHB star-rich Virgo overdensity. It is possible that *some* of these BHB stars are blue stragglers from Virgo, but there are two arguments that blue straggler contamination is not dominant. Firstly, the morphology of the BHB stars in the ~ 27 kpc slice in Fig. 4 argues strongly that most of the BHB star candidates are in fact BHB stars associated with Sagittarius — the distribution of BHB star candidates is elongated like the Sagittarius tidal stream, and extends past $l = 270$ where there are no stars in the Virgo overdensity (as can be seen in the ~ 11 kpc slice). Secondly, there are numerous blue stars along those lines of sight that are 1-2 mag fainter than the BHB stars we identify here; we interpret these numerous fainter blue stars as the blue straggler content of Virgo and Sagittarius (this is illustrated in Niederste-Ostholt et al. 2010 and Ruhland et al. 2010).

4. COMPARISON WITH MODELS OF STELLAR HALO FORMATION IN A COSMOLOGICAL CONTEXT

One motivation for this analysis was to test further the hypothesis that the stellar halo is composed of the debris from the disruption of dwarf galaxies. Cosmologically-motivated simulations of stellar halo formation such as those of Bullock & Johnston (2005) or Cooper et al. (2010) allow reasonably direct comparison of the observations and simulations. Bullock & Johnston (2005) have publicly released[5] the results of their simulations, including the luminosities, ages, metallicities, and element abundances of star particles (see also Robertson et al. 2005; Font et al. 2006) in eleven simulated stellar halos. Our main observational diagnostic, the spatially-varying ratio of MSTO to BHB stars, cannot be predicted directly by the models: while old and metal poor populations contain a significant population of BHB stars, it is not completely clear what the exact conditions are under which stellar populations are rich in BHB stars. An illustration of this challenge is the second-parameter problem: globular clusters with very similar metallicities can have very different horizontal branch morphologies, where it is unclear what parameter or parameters drive these variations (e.g., age or Helium content; see, e.g., Catelan 2009 for a discussion of this issue). Obviously, this uncertainty makes a correct BHB prescription impossible to implement.

Bearing in mind the practical difficulty of predicting the ratio between BHB and MSTO stars, we probe instead a metric that is better-defined in the models that gives some *qualitative* idea of population variations in stellar halos: stellar metallicity. We present in Fig. 5 a map of *r*-band luminosity-weighted stellar metallicity of three simulated stellar halos (Model numbers 4, 2, and 1 of Fig. 13 of Bell et al. 2008, corresponding to halo numbers 8, 5 and 2 respectively from Bullock & Johnston 2005) in the same distance bins as the observations (and convolved with the same absolute magnitude scatter of 0.9 mag as we use for the observations in Fig. 4). In order to produce this map, we have smoothed the most luminous star particles to reduce noise (although some noise in the maps is visible)[6]. The maps are luminosity-weighted (intensity scale), and color-coded by stellar metallicity (blue shows [Fe/H] = –1.5, red shows [Fe/H] = –0.5). The three halos were chosen to have differing amounts of substructure; model 4 (left) has a modest amount of substructure and model 1 (right) has prominent substructure, especially in the most distant bins. The key point to take away from Fig. 5 is that it clearly demonstrates the prediction that different substructures should have distinctive stellar populations (in this case parameterized by metallicity). This is in *qualitative* agreement with the observations — a quantitative match will be impossible to produce until the conditions under which BHB stars form are substantially better understood.

5. DISCUSSION

We have presented a map of spatial stellar population variations in the Milky Way's halo, using the ratio of BHB to MSTO stars. This map is reminiscent of analogous maps for M31 (McConnachie et al. 2009) and shows that descriptions of stellar halo populations in terms of radial gradients alone is an incomplete description of the data; much of the population variation is stream-like in morphology.

Our results may bear on the debate about the controversial nature and origin of the low-latitude structure: it may represent debris from a disrupted dwarf galaxy (e.g., Peñarrubia et al. 2005), or primarily consist of material stirred up from the outer disk of the Milky Way (see, e.g., Ibata et al. 2005; Momany et al. 2006; Kazantzidis et al. 2008, for discussion of this possibility). Fig. 4 shows the low-latitude structure to be almost devoid of BHB stars, implying in a broad sense a lack of metal-poor old populations. This is in contrast to many of the other halo substructures (at least parts of Sagittarius, Virgo, and Hercules/Aquila). If it is found in the future that the outer thin disk of the Milky Way is deficient in BHB stars, this may provide

[5] http://www.astro.columbia.edu/∼kvj/halos/

[6] In detail, we split star particles more luminous than 8 solar luminosities (sufficient to produce more than 1 MSTO star; Bell et al. 2008) into $L_r/8L_\odot$ particles, where L_r is the luminosity of the star particle of interest. In order to determine the placement of the new particles in 3D space, we find the nearest particles (between 100 and 1000 particles, depending on luminosity) drawn from the same satellite as the particle of interest (in order to preserve stream/satellite morphology) and distribute the new star particles in a space defined by these nearest neighbors. In practice, the details of this procedure are not critical for this application.

tentative support to the notion that the low-latitude structure is composed primarily of material stirred up from off the Milky Way's outer disk. At the very least, the lack of BHB stars (one of the few options for precise distance determination) is a significant practical challenge for those attempting to understand the 3-dimensional distribution of the low-latitude structure.

A feature of particular interest in Fig. 4 is the change in BHB content along the Sagittarius tidal stream. It is interesting to note that Niederste-Ostholt et al. (2010) argue for a constant BHB/MSTO ratio along the Sgr stream in the very region that we claim a significant difference in BHB/MSTO ratio (from $\sim 1/55$ to $\sim 1/80$). Niederste-Ostholt et al. (2010) subtract off the CMD of the region with the same b but $l_{\rm control} = 180 - l_{\rm Sgr}$, then count the number of MSTO stars and BHB stars left in the residual CMD. We have confirmed that the BHB/MSTO ratios of the control areas systematically change, from $\sim 1/50$ in the mirror region of the BHB star-rich part of Sgr, to $\lesssim 1/250$ in the mirror region of the BHB star-poor part of Sgr (this is apparent in Fig. 4; the top part of the last set of panels is relatively BHB-rich, whereas the lower parts of the last set of panels is poor in BHB stars both in Sgr and elsewhere). This change in the properties of the control sample drives the apparent constancy of the BHB/MSTO ratio in their work. It is not obvious (to us at least) how to properly interpret such a situation. From the perspective of an underlying smooth stellar halo (with abrupt changes in BHB/MSTO in the 'smooth' halo) with a superimposed stream, subtracting off the control fields is defensible. Yet, from the perspective of viewing the stellar halo as a combination of a number of structures in various stages of disruption, subtraction of a control field is less defensible, and would lead to artificial changes in the inferred properties of the structure of interest.

Viewed from the latter perspective, such a difference in the BHB/MSTO ratio would demonstrate that population gradients within a progenitor galaxy could in practice lead to population differences in the resulting tidal debris (a gradient in the Sagittarius tidal tail has been detected before using other stellar population diagnostics; e.g., Martínez-Delgado et al. 2004; Bellazzini et al. 2006; Chou et al. 2007). It may well be that the apparent abruptness of the change in the BHB/MSTO ratio between the Sagittarius debris in the anticenter direction and the NGP direction is because the debris streams in those directions were stripped from Sagittarius during different passages (see, e.g., Law et al. 2005 and Law & Majewski 2010 for models in which these two parts of the debris stream were stripped at significantly different times). Material closer to the edges of a satellite is preferentially stripped first; thus, in this interpretation we would hypothesize that the outermost parts of the Sagittarius dwarf galaxy were devoid of BHB stars, whereas the central parts of the dwarf were richer in BHB stars[7]. Spectroscopic follow-up of stream members, with the goal of weeding out phase-mixed stars from stars in a dynamically-cold stream, will help to differentiate between the two possible interpretations of the apparent population gradient in Sgr (see Keller, Yong & Da Costa 2010 for such an investigation of the Sgr trailing arm).

[7]It is worth noting that this picture may run counter to the scenario suggested by the observed differences in e.g., BHB to red clump star ratio, or metallicity, between the Sagittarius core and the tidal streams (Bellazzini et al. 2006; Chou et al. 2007). In their picture the core of Sagittarius is more metal-rich, and the tidal tail more metal poor. Here, we are sensitive to differences between different parts of the tidal tail; how that relates to earlier core/tail comparisons is not entirely clear.

6. CONCLUSIONS

In this paper, we have studied the spatial structure of stellar population variations in the stellar halo of the Milky Way. We made use of a new color selection method to isolate a sample of high-probability BHB star candidates, and compare their spatial density to that of color-selected MSTO stars (taken to represent the general stellar content of the halo). The abundance of BHB stars (vs. MSTO stars) is known to vary strongly among stellar populations with globular cluster-like ranges in age and metal abundance, where broadly speaking high BHB abundance signposts particularly old and metal-poor populations, and redder Horizontal Branch populations are characteristic of younger, more metal-rich populations, though the physical origin of such variations is currently debated. We mapped the relative distributions of BHB and MSTO stars across the Heliocentric distance range $5 \lesssim r/{\rm kpc} \lesssim 30$ for $\sim 1/4$ of the celestial sphere, providing a panoramic view of the content of the stellar halo.

We found large variations of the BHB/MSTO star ratio in the stellar halo. Most importantly, variations trace different previously-identified structures, indicating distinct populations and hence origins for them (in common, for example, with M31; McConnachie et al. 2009). Some halo features, e.g., the low-latitude structure, appear to be almost completely devoid of BHB stars, whereas other structures appear to be rich in BHB stars. The Sagittarius tidal stream shows an apparent variation in the BHB/MSTO ratio along its extent, which we interpret in terms of population gradients within the progenitor dwarf galaxy leaving observable signatures in our stellar halo. In a previous paper (Bell et al. 2008), we had shown that the level of density substructure in the Milky Way's stellar halo is consistent with models (e.g., Bullock & Johnston 2005) in which this component is built up exclusively from disrupted satellites. In this paper we have shown that another prediction of such models is qualitatively borne out: significant population variations, traced by the BHB/MSTO star ratio in the Milky Way's stellar halo, and with a spatial structure that correlates with the density substructures. This lends further observational support to the view that the stellar halo is predominantly assembled from the disrupted debris of dwarf galaxies.

We thank the referee for their helpful suggestions. We wish to thank Jorge Penarrubia and Frank van den Bosch for useful discussions. C. R. was supported by the Emmy Noether Programme of the Deutsche Forschungsgemeinschaft, and is a member of the Heidelberg International Max Planck Research School program. D. W. H. is a research fellow of the Alexander von Humboldt Foundation of Germany.

Funding for the SDSS has been provided by the Alfred P. Sloan Foundation, the Participating Institutions, the National Aeronautics and Space Administration, the National Science Foundation, the U.S. Department of Energy, the Japanese Monbukagakusho, and the Max Planck Society. The SDSS Web site is http://www.sdss.org/.

The SDSS is managed by the Astrophysical Research Consortium (ARC) for the Participating Institutions. The Participating Institutions are The University of Chicago, Fermilab, the Institute for Advanced Study, the Japan Participation Group, The Johns Hopkins University, Los Alamos National Laboratory, the Max-Planck-Institute for Astronomy (MPIA), the Max-Planck-Institute for Astrophysics (MPA), New Mexico State University, University of Pittsburgh, Princeton University, the United States Naval Observatory, and the University

of Washington.

REFERENCES

Abadi, M. G., Navarro, J. F., & Steinmetz, M. 2006, MNRAS, 365, 747
Abazajian, K. N., et al. 2009, ApJS, 182, 543
Bell, E. F., et al. 2008, ApJ, 680, 295
Bellazzini, M., Correnti, M., Ferraro, F. R., Monaco, L., & Montegriffo, P. 2006a, A&A, 446, L1
Bellazzini, M., Newberg, H. J., Correnti, M., Ferraro, F. R., & Monaco, L. 2006, A&A, 457, L21
Belokurov, V., et al. 2007a, ApJ, 657, L89
Belokurov, V., et al. 2007b, ApJ, 658, 337
Belokurov, V., et al. 2006, ApJ, 642, L137
Blanton, M. R., Lin, H., Lupton, R. H., Maley, F. M., Young, N., Zehavi, I., & Loveday, J. 2003, AJ, 125, 2276
Bramich, D. M., et al. 2008, MNRAS, 386, 887
Brown, T. M., Smith, E., Ferguson, H. C., Rich, R. M., Guhathakurta, P., Renzini, A., Sweigart, A. V., & Kimble, R. A. 2006, ApJ, 652, 323
Bullock, J. S., & Johnston, K. V. 2005, ApJ, 635, 931
Bullock, J. S., Kravtsov, A. V., & Weinberg, D. H. 2001, ApJ, 548, 33
Carney, B. W., Latham, D. W., Laird, J. B., Grant, C. E., & Morse, J. A. 2001, AJ, 122, 3419
Carollo, D., et al. 2007, Nature, 450, 1020
Catelan, M. 2009, Ap&SS, 320, 261
Chou, M.-Y., et al. 2007, ApJ, 670, 346
Clewley, L., Warren, S. J., Hewett, P. C., Norris, J. E., Peterson, R. C. & Evans, N. W. 2002, MNRAS, 337, 87
Clewley, L., Warren, S. J., Hewett, P. C., Norris, J. E., Wilkinson, M. I. & Evans, N. W. 2005, MNRAS, 362, 349
Cooper, A. P., et al. 2010, MNRAS, 406, 744
de Jong, J. T. A., Yanny, B., Rix, H.-W., Dolphin, A. E., Martin, N. F., & Beers, T. C. 2010, ApJ, 714, 663
Dotter, A., Chaboyer, B., Jevremović, D., Baron, E. & Ferguson, J. W., Sarajedini, A. & Anderson, J. 2007, AJ, 134, 376
Dotter, A., Chaboyer, B., Jevremović, D., Kostov, V., Baron, E. & Ferguson, J. W. 2008, ApJS, 178, 89
Duffau, S., Zinn, R., Vivas, A. K., Carraro, G., Méndez, R. A., Winnick, R., & Gallart, C. 2006, ApJ, 636, L97
Font, A. S., Johnston, K. V., Bullock, J. S., & Robertson, B. E. 2006, ApJ, 638, 585
Fukugita, M., Ichikawa, T., Gunn, J. E., Doi, M., Shimasaku, K., & Schneider, D. P. 1996, AJ, 111, 1748
Grillmair, C. J. 2006, ApJ, 645, L37
—. 2009, ApJ, 693, 1118
Grillmair, C. J., & Dionatos, O. 2006, ApJ, 643, L17
Grillmair, C. J., & Johnson, R. 2006, ApJ, 639, L17
Gunn, J. E., et al. 1998, AJ, 116, 3040
Gunn, J. E., et al. 2006, AJ, 131, 2332
Helmi, A., Navarro, J. F., Nordström, B., Holmberg, J., Abadi, M. G., & Steinmetz, M. 2006, MNRAS, 365, 1309
Hills, J. G. & Day, C. A. 1976, Astrophysics Letters, 17, 87
Hogg, D. W., Finkbeiner, D. P., Schlegel, D. J., & Gunn, J. E. 2001, AJ, 122, 2129
Hoyle, F. & Schwarzschild, M. 1955, ApJS, 2, 1
Ibata, R., Chapman, S., Ferguson, A. M. N., Lewis, G., Irwin, M., & Tanvir, N. 2005, ApJ, 634, 287
Ibata, R., Martin, N. F., Irwin, M., Chapman, S., Ferguson, A. M. N., Lewis, G. F., & McConnachie, A. W. 2007, ApJ, 671, 1591
Ibata, R. A., Gilmore, G., & Irwin, M. J. 1995, MNRAS, 277, 781
Ibata, R. A., Irwin, M. J., Lewis, G. F., Ferguson, A. M. N., & Tanvir, N. 2003, MNRAS, 340, L21
Ivezić, Ž., et al. 2004, Astronomische Nachrichten, 325, 583
Ivezić, Ž., et al. 2008, ApJ, 684, 287
Jurić, M., et al. 2008, ApJ, 673, 864
Kazantzidis, S., Bullock, J. S., Zentner, A. R., Kravtsov, A. V., & Moustakas, L. A. 2008, ApJ, 688, 254
Keller, S. C., Yong, D. & Da Costa, G. S. 2010, ApJ, 720, 940
Kinman, T. D., Suntzeff, N. B. & Kraft, R. P. 1994, AJ, 108, 1722
Kinman, T. D., Salim, S. & Clewley, L. 2007, ApJ, 662, L111
Knigge, C., Leigh, N. & Sills, A. 2009, Nature, 457, 288
Law, D. R., Johnston, K. V., & Majewski, S. R. 2005, ApJ, 619, 807
Law, D. R. & Majewski, S. R. 2010, ApJ, 714, 229
Lupton, R. H., Gunn, J. E., & Szalay, A. S. 1999, AJ, 118, 1406
Majewski, S. R., Skrutskie, M. F., Weinberg, M. D., & Ostheimer, J. C. 2003, ApJ, 599, 1082
Martínez-Delgado, D., Gómez-Flechoso, M. Á., Aparicio, A., & Carrera, R. 2004, ApJ, 601, 242
Matheiu, R. D., & Geller, A. M. 2009, Nature, 462, 1032
McConnachie, A. W. et al. 2009, Nature, 461, 66
McCrea, W. H. 1964, MNRAS, 128, 147
Momany, Y., Zaggia, S., Gilmore, G., Piotto, G., Carraro, G., Bedin, L. R., & de Angeli, F. 2006, A&A, 451, 515
Niederste-Ostholt, M., Belokurov, V., Evans, N. W. & Peñarrubia, J. 2010, ApJ, 712, 516
Newberg, H. J., Yanny, B. & Willett, B. A. 2009, ApJ, L700, 61
Newberg, H. J., et al. 2007, ApJ, 668, 221
Newberg, H. J., et al. 2002, ApJ, 569, 245
Odenkirchen, M., et al. 2001, ApJ, 548, L165
Peñarrubia, J., et al. 2005, ApJ, 626, 128
Perets, H. B. & Fabrycky, D. C. 2009, ApJ, 697, 1048
Pier, J. R., Munn, J. A., Hindsley, R. B., Hennessy, G. S., Kent, S. M., Lupton, R. H., & Ivezić, Ž. 2003, AJ, 125, 1559
Preston, G. W. & Sneden, C. 2000, AJ, 120, 1014
Richardson, J. C., et al. 2008, AJ, 135, 1998
Robertson, B., Bullock, J. S., Font, A. S., Johnston, K. V., & Hernquist, L. 2005, ApJ, 632, 872
Ruhland, C., Bell, E. F., Rix, H.-W. & Xue, X. X. 2010, submitted to ApJ
Sandage, A. R. 1953, AJ, 58, 61
Sirko, E., et al. 2004, AJ, 127, 899
Smith, J. A., et al. 2002, AJ, 123, 2121
Stoughton, C., et al. 2002, AJ, 123, 485
Strauss, M. A., et al. 2002, AJ, 124, 1810
Tucker, D. L., et al. 2006, Astronomische Nachrichten, 327, 821
Tumlinson, J. 2010, ApJ, 708, 1398
Wilhelm, R., Beers, T. C. & Gray, R. O. 1999, AJ, 117, 2308
Xue, X. X., et al. 2008, ApJ, 684, 1143
Yanny, B., et al. 2003, ApJ, 588, 824

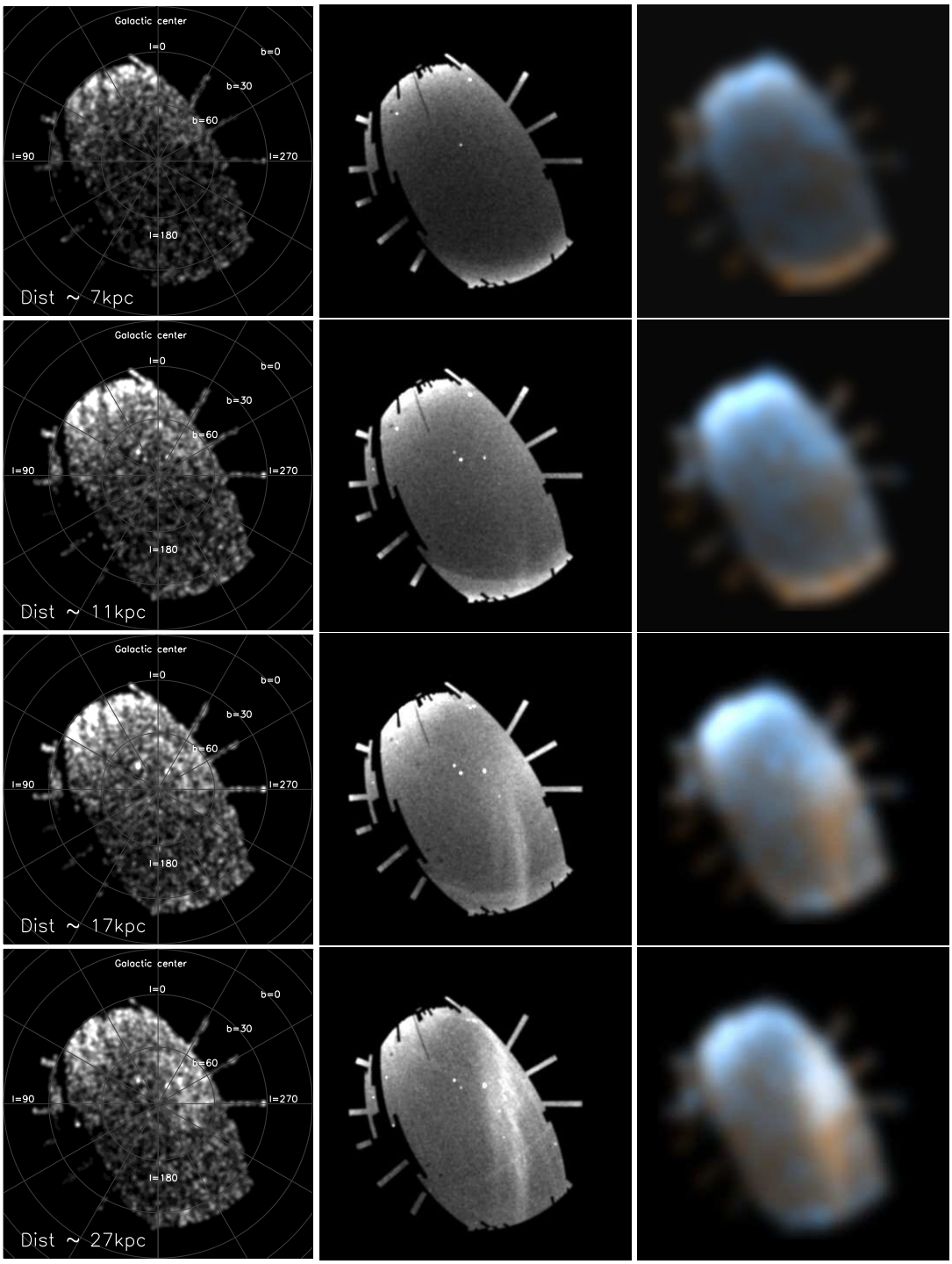

FIG. 4.— Left: Map of the BHB stars in thick distance modulus slices, where the BHB distances have been 'degraded' to $\sigma_M = 0.9$ to match the distance resolution of MSTO stars. Middle: Map of MSTO stars in the same distance modulus slice, assuming a MSTO $M_r = 4.5$. Right: Color representation of the BHB/MSTO ratio, smoothed with a 6 degree Gaussian. Panels are arranged in order of increasing distance modulus from top to bottom, $13.5 \leq m-M < 14.5$, $14.5 \leq m-M < 15.5$, $15.5 \leq m-M < 16.5$, and $16.5 \leq m-M < 17.5$, or distances of $5-8$, $8-13$, $13-20$ and $20-32$ kpc respectively. In all panels, a gray scale that varies linearly with the star number is used.

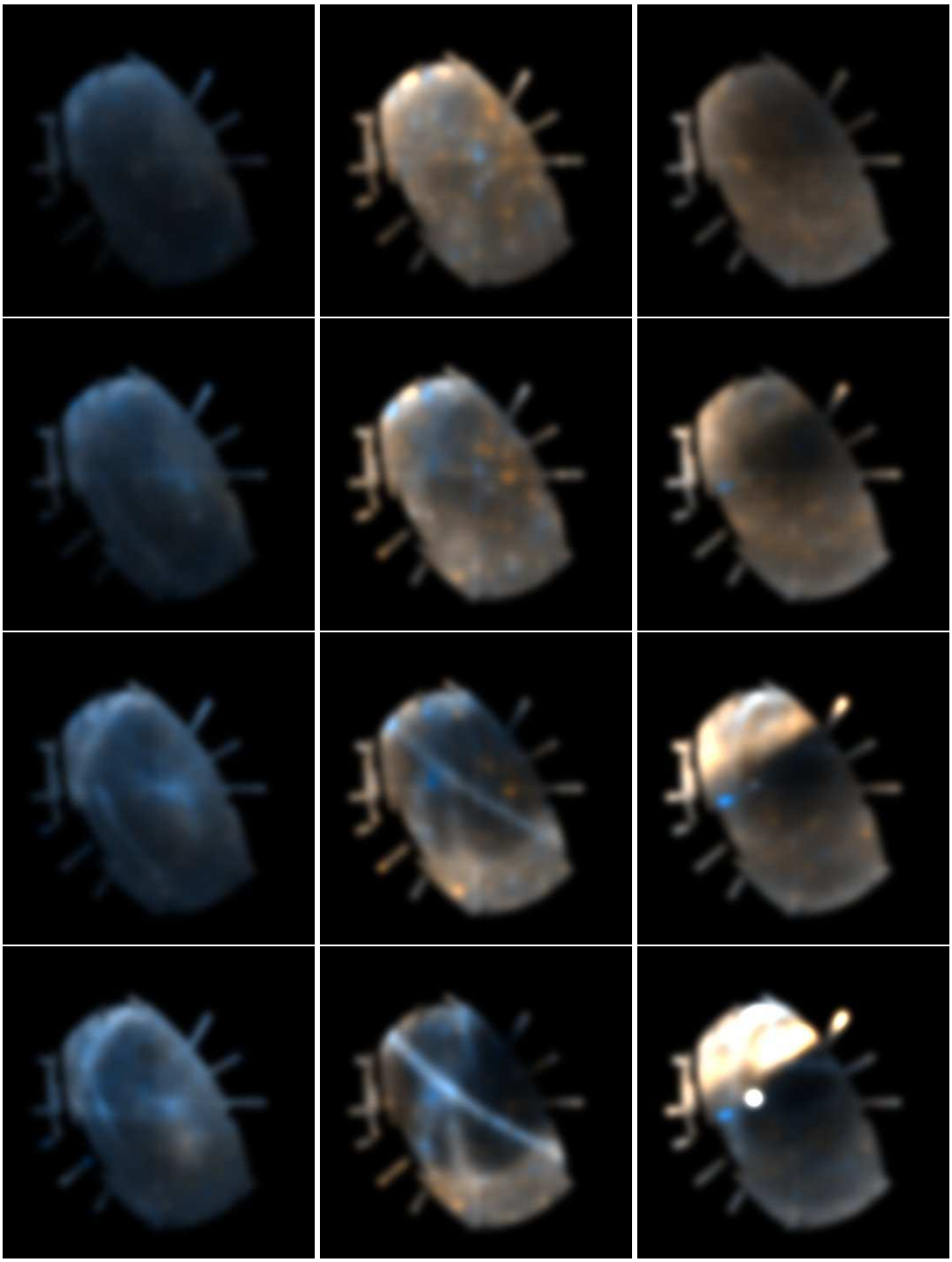

FIG. 5.— A color representation of the relationship between structure and metallicity in simulated stellar halos of Bullock & Johnston (2005). The three columns show stellar halos with relatively low, average, and large amounts of substructure. The 4 rows show the simulated halos convolved with the MSTO absolute magnitude distribution and split into the same distance bins as used for the SDSS data: $13.5 \leq m-M < 14.5$, $14.5 \leq m-M < 15.5$, $15.5 \leq m-M < 16.5$, and $16.5 \leq m-M < 17.5$, or distances of $5-8$, $8-13$, $13-20$ and $20-32$ kpc respectively. The intensity scale is linear and scales with the number of stars; the color scale shows metallicity, where blue denotes [Fe/H] = –1.5 and red denotes [Fe/H] = –0.5.